

# Estimation of dynamic joint torques and trajectory formation from surface electromyography signals using a neural network model

Yasuharu Koike\*, Mitsuo Kawato

Department 3, ATR Human Information Processing Research Laboratories, 2-2 Hikaridai, Seika-cho, Soraku-gun, Kyoto 619-02, Japan

Received: 24 August 1994/Accepted in revised form: 25 April 1995

**Abstract.** In this study, human arm movement was reconstructed from electromyography (EMG) signals using a forward dynamics model acquired by an artificial neural network within a modular architecture. Dynamic joint torques at the elbow and shoulder were estimated for movements in the horizontal plane from the surface EMG signals of 10 flexor and extensor muscles. Using only the initial conditions of the arm and the EMG time course as input, the network reliably reconstructed a variety of movement trajectories. The results demonstrate that posture maintenance and multijoint movements, entailing complex via-point specification and co-contraction of muscles, can be accurately computed from multiple surface EMG signals. In addition to the model's empirical uses, such as calculation of arm stiffness during motion, it allows evaluation of hypothesized computational mechanisms of the central nervous system such as virtual trajectory control and optimal trajectory planning.

## 1 Introduction

Over the years, the neurophysiology and biomechanics of muscle systems have been investigated quite extensively in order to characterize the relations between muscle activity (electromyography, EMG) and various dynamical and/or kinematic aspects of the ensuing movement behavior. There have been numerous efforts to correlate the duration, magnitude, and timing of phasic EMG bursts with the amplitude, duration, and maximum speed of limb motion (Gottlieb et al. 1989; Brown and Cooke 1990; Karst and Hasan 1991). Although the complexity of musculoskeletal systems has made it difficult to reconstruct movement accurately from EMG signals, this goal

is central to efforts to model motor control mechanisms of the central nervous system (CNS) computationally.

For example, quantitative dynamic models of the arm and muscle force generation have been used to predict muscle tension and/or motion from EMG signals (Akazawa et al. 1988; Wood et al. 1989; Winters 1990; Clancy and Hogan 1991). Typically, these models have been based on the spring-like properties of muscles: Muscle tension can be derived by controlling muscle length and activation level (Rack and Westbury 1969). It was hoped that piecemeal examination of the basic dynamical parameters would result in progressively better quantitative models of the musculoskeletal system (i.e., muscle model, neural model, skeletal system model with variable muscle moment arms, Lagrangian dynamics model of the arm). To this end, our group earlier proposed a 6-muscle human arm model (Katayama and Kawato 1993) and a 17-muscle monkey arm model (Dornay et al. 1992). A problem with this approach, however, is that assumptions have to be made at each step about the largely unknown nonlinear properties of the musculoskeletal and nervous systems.

The aim of the current study was to construct a complete forward dynamics model (FDM) of the human arm that affords accurate estimation of movement trajectories from the input of physiological signals such as muscle EMG. To achieve this, we used an artificial neural network that learned nonlinear functions relating physiological recordings of EMG signals to simultaneous measurement of two-joint planar movement trajectories. Previously, we have used surface EMG signals to estimate: (1) joint torques under isometric conditions in the horizontal plane (Koike et al. 1993); (2) three-dimensional posture (three degrees-of-freedom at the shoulder and one degree-of-freedom at the elbow) (Koike and Kawato 1994a); and (3) joint angular acceleration with subsequent reconstruction of movement trajectories in the horizontal plane (Koike and Kawato 1994b).

The model developed here incorporated the following as domain-specific information: (1) the relationship between the EMG input signal and quasi-tension, (2) the dynamics of the arm, and (3) nonlinear muscle properties.

Correspondence to: Y. Koike

\*Present address: Toyota Motor Corporation, Future Project Division No.1, Bioresearch Laboratory, 1 Toyota-cho, Toyota, Aichi 471-71, Japan

To implement (1), a network was prepared to act as a temporal finite impulse response (FIR) filter. For (2), the physical parameters of the subject arm were calculated from the measured three-dimensional (3D) shape of the arm, and the arm dynamics were described by Lagrange equations. To efficiently implement (3), various nonlinear properties of the musculoskeletal system were obtained through training of the modular network.

In Sect. 2 of this paper, we describe how these three domains of knowledge were incorporated into our model. Section 3 outlines the procedures used to collect and process the experimental data. Section 4 shows simulation results for joint torque estimation and trajectory formation using the obtained neural network. In Sect. 5, we discuss the reliability of the model and the directions of further development.

**2 The model which estimates trajectories from surface EMG signals**

Figure 1 compares a view of information flow in a human (A) to the computational procedure adopted in this paper (B). Figure 1A shows a process of transformation from motor commands to a trajectory. The CNS first sends a command to the muscles, causing them to exert tension. Nonlinear relationships exist between muscle-exerted tension and motor commands. Muscle tension is related to motor command (firing rate) through a sigmoid function (Rack and Westbury 1969; Mannard and Stein 1973). This nonlinearity is caused not only by the firing-rate-tension relationship but also by recruitment of  $\alpha$ -motor neurons. Moreover, there are two nonlinear relationships: between muscle tension and muscle length, and between muscle tension and muscle contractile velocity (Fig. 1A) (Basmajian and De Luca 1985). One is called the length-tension curve, which describes how muscle tension increases with length even if the motor command does not change. The other is called the velocity-tension curve and describes how muscle tension decreases with contractile velocity for a constant motor command.

The joint torque is then calculated from the muscle tension and muscle moment arms. The distance between the joint axis and the force action line of the muscle is the muscle moment arm. The moment arm changes nonlinearly depending on the joint angle and because muscles wrap around other muscles, bones, and connective tissues. Joint torque is produced as the difference between agonist and antagonist muscle torques, which depend on the muscle tension and the muscle moment arm. Arm dynamics exist between the joint torque and the joint angle, velocity, and acceleration. Understanding the dynamics, however, is difficult because of the presence of complex, nonlinear interaction forces among the moving joint segments.

Our aim has been to construct a forward model of the human arm using data obtained from physiological measurements. This model took the EMG signal as input and produced end-point trajectories as output. Figure 1B shows the current procedure employed to compute end-point trajectories from EMG signals. We have been able

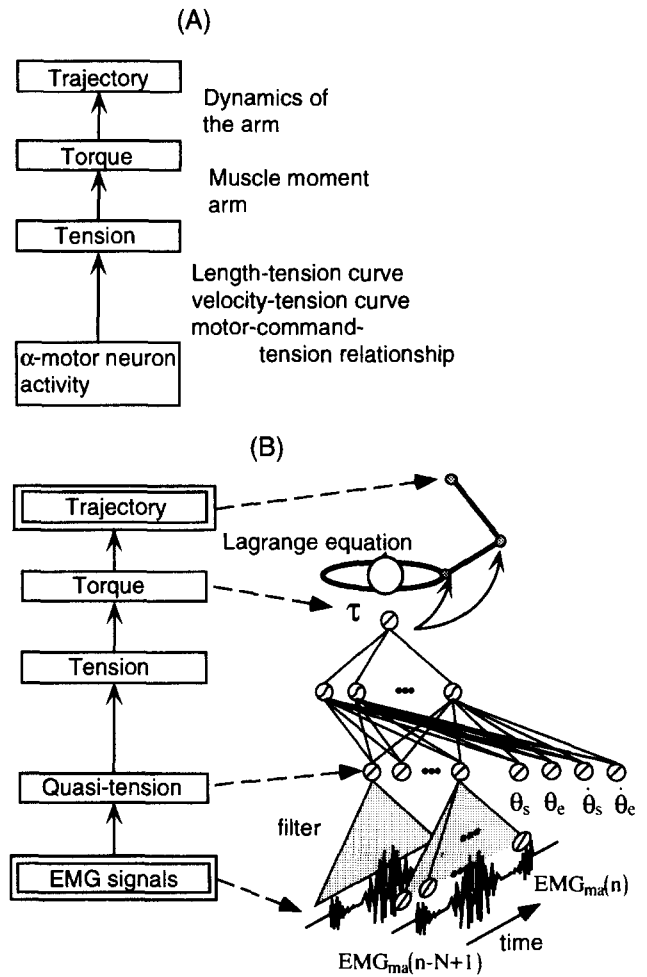


**Fig. 1.** Comparison of the information flow in the organism (A) to the computational procedure adopted in this paper (B). In (A), control signals from the central nervous system (CNS) are sent to each muscle via  $\alpha$  motor neurons. The signals activate the muscles (muscle tension), the contraction causes joint torques, and then the arm moves along movement trajectories according to the arm dynamics. In (B), we can measure electromyography (EMG) signals and trajectory; they both have a double-line box around them. EMG signals, though temporally and spatially distorted, reflect the motor commands fed to the muscles. Since we cannot measure motor neuron activity directly, though not ideal, we will treat the low-pass-filtered EMG activity as a substitute for the firing rate of motor neurons

to measure the behavior of EMG signals and trajectories of the hand, elbow, and shoulder (measured quantities are shown with a double-line box around them). We treat EMG signals as a record of the motor commands to the muscles, since we cannot directly measure the motor neuron activity. Though not ideal, EMG activity is a reasonable reflection of the firing rate of a motor neuron. Actual EMG activity was transformed by a linear, second-order, low-pass filter. The transformed signal is called 'quasi-tension,' because it seems to be highly correlated with the true muscle tension. We also used a neural network with a modular architecture to convert quasi-tension to estimated dynamic torque. If a single, multi-layer network performs different tasks under different occasions, there will generally be strong interference

effects which lead to slow learning and poor generalization. If we know in advance that a set of training cases may be naturally divided into subsets that correspond to distinct subtasks, interference can be reduced by using a modular architecture. From the physiological viewpoint, this division is natural. Muscle has nonlinear properties, such as the length-tension relationship and velocity-tension relationship. In the case of movement, both nonlinear properties have to be considered. In the case of posture control, however, the velocity-tension relationship does not need to be considered. It is also widely known that the dynamic characteristics of spinal and supraspinal reflex loops differ greatly between movement and posture maintenance. In this part, the neural network learned nonlinear muscle properties, such as the length-tension curve and the velocity-tension curve, and nonlinear properties of musculoskeletal systems, such as the muscle moment arms. We did this by using actual torques as teaching signals and actual joint kinematics as additional inputs. The actual joint kinematics were obtained from the measured cartesian trajectories of the joints. The teaching torque signal was computed using the actual joint angle kinematics and the measured physical parameters of the arm using inverse dynamics equations. Finally, the estimated torques and the actual joint kinematics were used to estimate joint angle acceleration using the forward dynamics equations. These angular accelerations were integrated to predict the next-time-step joint state, and end-point trajectories were estimated using forward kinematics equations. In this manner, we were able to construct a forward model that transformed EMG signals at the current time step to end-point trajectories at the next time step. The following details each step.

### 2.1 The relationship between EMG signals and quasi-tensions

Surface EMG signals are spatiotemporally convoluted action potentials of the muscle membranes and involve not only descending central motor commands but also reflex motor commands generated from sensory feedback signals. There have been considerable efforts to estimate muscle force from surface EMG signals (Basmajian and De Luca 1985; Akazawa et al. 1988; Wood et al. 1989; Clancy and Hogan 1991). From these previous studies in medical electronics and biological engineering (Basmajian and De Luca 1985), it can be expected that low-pass-filtered EMG signals (quasi-tension) reflect the firing rate of  $\alpha$  motor neurons as high-frequency components of EMG reflect the shape of individual action potentials, while low-frequency components reflect the firing-frequency of motor nerve fibers. In neurophysiological studies, it was found that a second-order, low-pass filter was sufficient for estimating muscle forces from the nerve impulse train (Mannard and Stein 1973). The relationship between the EMG input signal and  $\hat{T}$  (quasi-tension) the output signal can be represented as an FIR filter,

$$\hat{T}(t) = \sum_{j=1}^n h_j \cdot EMG(t - j + 1) \quad (1)$$

where  $h_j$  is the filter,  $EMG$  represents EMG signals,  $\hat{T}$  represents 'quasi-tensions', and  $j$  is the number of discrete time.  $EMG$  is actually the digitally rectified, integrated, and filtered signal. The second-order frequency response of the filter  $H(s)$  is represented as follows:

$$H(s) = \frac{\omega_n^2}{(s^2 + \zeta\omega_n s + \omega_n^2)} \quad (2)$$

where  $\omega_n$  and  $\zeta$  denote natural frequency and damping coefficient, respectively. The impulse response of the function in (2) is

$$h(t) = a \times (\exp^{-bt} - \exp^{-ct}) \quad (3)$$

The coefficients  $h_j$  in (1) can be acquired by digitizing  $h(t)$  with the given coefficients  $a$ ,  $b$ , and  $c$ .

### 2.2 The relationship between quasi-tensions and joint torques

Each joint torque was estimated from quasi-tension, joint angle, and velocity using an artificial neural network model with a modular architecture as shown in Fig. 2 for the shoulder network. The modular architecture consists of two types of networks: expert and gating networks (Jacobs and Jordan 1991; Nowlan and Hinton 1991). Two modular shoulder and elbow networks were used to estimate the two joint torques respectively in order to improve the accuracy of the torque estimation.

#### 2.2.1 Modular learning

We briefly illustrate the modular learning algorithm which was proposed by Jacobs and Jordan (1991) and

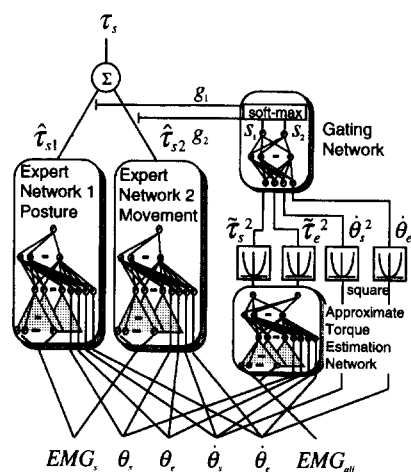


Fig. 2. Structure of the artificial neural network which estimates the shoulder joint torque using a modular architecture.  $EMG_s$  is the EMG signals of muscles related to the shoulder movement.  $EMG_{all}$  is the EMG signals of all muscles.  $\hat{\tau}_s^2$  and  $\hat{\tau}_e^2$  are the square of the approximate torque of the shoulder and elbow, respectively, calculated by the approximate torque estimation network.  $\hat{\tau}_{s1}$  and  $\hat{\tau}_{s2}$  are shoulder joint torques estimated by the expert network 1 and 2, respectively. See (4) for  $g_1$  and  $g_2$

Nowlan and Hinton (1991) and used in this study. The  $j$ th output of the gating network,  $g_j$ , is calculated by the following soft-max function

$$g_j = \frac{e^{s_j}}{\sum_{i=1}^N e^{s_i}} \quad (4)$$

where  $s_i$  is calculated from the input signals to the gating network, and  $N$  denotes the number of outputs. The total output of the modular network is as follows:

$$\tau = \sum_{i=1}^N g_i \hat{\tau}_i \quad (5)$$

where  $\hat{\tau}_i$  is the output of the  $i$ th expert network.

The gating and expert networks are trained to maximize the following log-likelihood function:

$$\ln L = \ln \sum_{i=1}^N g_i e^{-\frac{\|\tau - \hat{\tau}_i\|^2}{2\sigma_i^2}} \quad (6)$$

where  $\sigma_i$  is the variance scaling parameter of the  $i$ th expert network.

The adaptation rules of the weights in the gating network are derived from the partial derivative of (6) by applying the chain rule.

$$\frac{\partial \ln L}{\partial s_i} = h_i - g_i \quad (7)$$

where  $h_i$  is defined by the following equation corresponding to the posterior probability.

$$h_i = \frac{g_i e^{-\frac{\|\tau - \hat{\tau}_i\|^2}{2\sigma_i^2}}}{\sum_{j=1}^N g_j e^{-\frac{\|\tau - \hat{\tau}_j\|^2}{2\sigma_j^2}}} \quad (8)$$

Similarly, the adaptation rules of the weights in the expert networks are derived from the partial derivative of (6) by applying the chain rule.

$$\frac{\partial \ln L}{\partial \hat{\tau}_i} = h_i \frac{\tau - \hat{\tau}_i}{\sigma_i^2} \quad (9)$$

### 2.2.2 A neural network that estimates each joint torque

In Fig. 2, each expert network estimated shoulder joint torque. For the case of elbow joint torque, the same modular architecture was used except that the expert input signals were  $EMG_e$ : the EMG signals of muscles related to the elbow joint movements. The expert network 1 estimated joint torques  $\hat{\tau}_{s1}$  mainly during posture control, and the expert network 2 estimated joint torques  $\hat{\tau}_{s2}$  mainly during movements. This division of their roles was first attained by pre-training and further refined by the automatic modular learning algorithm.

The gating network switched the expert networks by judging whether the arm moved or not. To judge whether the arm moved or not, the square of the angular velocity and torques which change faster than velocity signals were used. To calculate this torque input, an approximate torque estimation network was prepared at the input side of the gating network (Fig. 2).

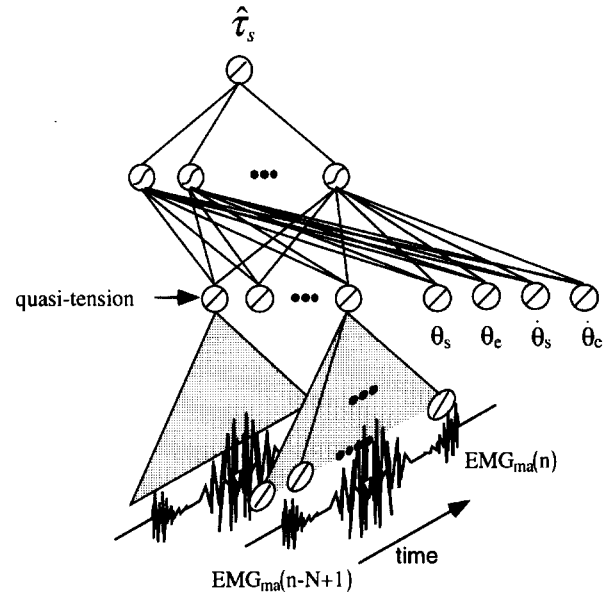


Fig. 3. One of the expert neural networks which estimate the shoulder joint torque. The approximate torque estimation network also has a similar structure except that it has two output units for the shoulder and elbow torques

Each expert network consisted of a four-layer network, as shown in Fig. 3. The first-layer inputs of this four-layer network were the EMG signals recorded from some of the 10 muscles over a 0.5-s interval. The EMG signals from double-joint muscles, related single-joint muscles, the joint angle, and the joint angular velocity of the elbow and shoulder were the expert network inputs. The number of units in the second layer was 11 for the shoulder expert network and 9 for the elbow expert network. The calculation of the 'quasi-tension' from the EMG signals was implemented in the expert network between the first and the second layers. In a strict sense, 'quasi-tension', a linearly filtered EMG signal, cannot represent muscle tension. Because the FIR filter is linear, the nonlinear muscle properties found in the motor-command-tension, length-tension, and velocity-tension curves are not represented between the first and second layers. Thus, the network learns these nonlinear properties between the second and the fourth layers. The second-layer inputs were the joint angles and joint angular velocities of the elbow and shoulder, as well as the quasi-tensions. The third layer consisted of 30 hidden units. The fourth, the output layer, estimated the joint torque. Activation functions, relating the weighted sum of synaptic inputs to the output of an artificial neuron model, of only the third layer are the nonlinear sigmoid functions.

The gating network consisted of a three-layer network. The first-layer inputs were the square of each joint torque and joint velocity. Thus, the number of units in the first layer was four ( $2 \times 2$ ). The second layer consisted of 10 hidden units. The third, the output layer, consisted of two units which calculate  $s_j$  in (4) corresponding to two expert networks ( $j = 1, 2$ ). Again, only the second layer

units are nonlinear. The outputs of the gating network are  $g_1$  and  $g_2$  as defined in (4).

The approximate torque estimation network also consisted of a four-layer network like the expert networks shown in Fig. 3. The first-layer inputs were the EMG signals from all 10 muscles over a 0.5-s interval. The second-layer inputs were the joint angles and joint angular velocities of the elbow and shoulder, as well as the 10 quasi-tensions. Thus, the number of units in the second layer is 14. The number of units in the third layer is 30. The fourth, the output layer, consisted of two units which estimated shoulder and elbow joint torques  $\tilde{\tau}_s$  and  $\tilde{\tau}_e$ . Again, only the third layer is nonlinear. This network had less accuracy than the expert networks, but it could provide sufficiently good information to judge whether the arm moved or not. The training method of the approximate torque estimation network was standard. The actual torques  $\tau_s$  and  $\tau_e$  are given as the teaching signals, and the objective function is defined as the squared sum of the difference between real and estimated joint torques.

### 2.3 The relationship between joint torques and trajectories

In this paper, we deal with horizontal planar movements of the shoulder joint and the elbow joint (flexion-extension) at the shoulder level. Therefore, the controlled object is the two-link system comprised of the upper arm (link 1) and forearm (link 2) shown in Fig. 4. We use the following dynamics equations for two-joint horizontal movements of the upper arm and the forearm:

$$\begin{aligned} & (I_1 + I_2 + 2M_2L_1l_{g2}\cos\theta_e + M_2L_1^2)\ddot{\theta}_s \\ & + (I_2 + M_2L_1l_{g2}\cos\theta_e)\ddot{\theta}_e \\ & - M_2L_1l_{g2}(2\dot{\theta}_s + \dot{\theta}_e)\dot{\theta}_e\sin\theta_e = \tau_s \\ & (I_2 + M_2L_1l_{g2}\cos\theta_e)\ddot{\theta}_s + I_2\ddot{\theta}_e \\ & + M_2L_1l_{g2}(\dot{\theta}_s)^2\sin\theta_e = \tau_e \end{aligned} \quad (10)$$

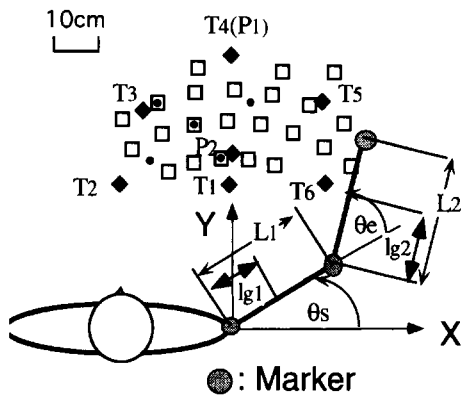


Fig. 4. Experimental settings and definitions of joint angles and link physical parameters of the two-link arm model.  $L_1$ , length of upper arm;  $L_2$ , length of forearm;  $l_{g1}$ , distance from the center of mass of upper arm to the shoulder joint;  $l_{g2}$ , distance from the center of mass of forearm to the elbow joint;  $\theta_s$ , shoulder joint angle;  $\theta_e$ , elbow joint angle. Black circles show 5 points where the subject exerted isometric hand forces in experiment 1. Black diamonds show the start, via, and target points of movements in experiment 2. White squares show 23 points where postures are maintained in experiment 3

where  $\tau$ ,  $\theta$ ,  $\dot{\theta}$ ,  $\ddot{\theta}$  represent the joint torque, joint angle, velocity, and acceleration, respectively.  $M_i$ ,  $L_i$ ,  $l_{gi}$ ,  $I_i$  represent the mass, length, distance from the center of mass to the joint axis, and rotary inertia around the joint for each link, respectively.

When the problem is to find the joint motion corresponding to a known sequence of input torques, the transformation (10) is referred to as forward dynamics. If the initial conditions (joint angles and velocities) and the control signals (joint torques from the initial time to the final time) are given, then the time course of  $\theta$  and  $\dot{\theta}$  are obtained by numerical integration of the dynamics equations (10).

When the problem is to find the joint torques corresponding to the desired time sequence of joint angles, the transformation (10) is referred to as inverse dynamics. In the experimental procedure of this paper, to calculate the joint torques from measured trajectories, the dynamics equations (10) are also used. In the case of forward dynamics, the information flows from the right side of (10), and in the case of inverse dynamics, the information flows from left to right.

## 3 Experimental procedures

### 3.1 Experiment 1: isometric force generation

One healthy subject, 29 years old, participated in this study. The seated subject's shoulder was restrained by a harness. In the first experiment, to analyze the relationship between EMG signals and quasi-tension, the forces generated at the hand under isometric conditions and surface EMG signals were measured.

His wrist was secured by a cuff and supported horizontally using the beam which was attached to a force-torque sensor. The subject was trained first to exert a hand force of about 50% maximum. The subject exerted isometric hand forces in two different directions: forward and backward, left and right, at five different locations ( $\theta_e, \theta_s$ ) of  $(30^\circ, 110^\circ)$ ,  $(40^\circ, 80^\circ)$ ,  $(50^\circ, 90^\circ)$ ,  $(60^\circ, 100^\circ)$ , or  $(70^\circ, 70^\circ)$  indicated by the black circles in Fig. 4. These trials lasted for seven seconds and involved various rates of force production. At each of the 5 positions, the subject made two attempts in each direction. Thus, the rate of the hand-force change was intentionally varied, and the peak magnitude was roughly controlled.

The hand force was measured by a force-torque sensor and filtered at an upper cut-off frequency of 130 Hz in hardware. These signals were first sampled at 2000 Hz with 12-bit resolution and were then re-sampled at 200 Hz. The positions of the hand, elbow, and shoulder were recorded at 400 Hz using the OPTOTRAK position sensing system. The shoulder and elbow joint angles were calculated from those position data. The joint angle data were digitally filtered at an upper cut-off frequency of 10 Hz by a Butter-worth filter. Then, they were re-sampled at 200 Hz. The shoulder and elbow joint torques were calculated from the measured hand force within the horizontal plane (two degrees-of-freedom)

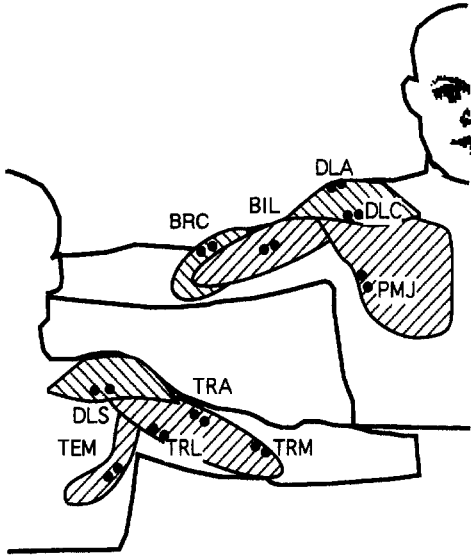


Fig. 5. Electrode positions in EMG measurement. See text for muscle name abbreviations

multiplied by the transpose of the jacobian of the coordinate transformation.

EMG signals were recorded from the 10 muscles shown in Fig. 5. For flexion/extension of the shoulder joint, the deltoid-clavicular part (DLC), deltoid-acromial part (DLA), deltoid-scapular part (DLS), pectoralis major (PMJ), and teres major (TEM) were measured. For double-joint muscles, the biceps-long head (BIL) and triceps-long head (TRL) were measured. For flexion/extension of the elbow joint, the brachialis (BRC), triceps-medial head (TRM), and triceps-lateral head (TRA) were measured.

The EMG signals were recorded using a pair of silver-silver chloride surface electrodes in a bipolar configuration. The electrodes each had a 10-mm diameter and were separated by approximately 15 mm. Test maneuvers were used to verify electrode placement. Each signal was sampled at 2000 Hz with 12-bit resolution. This signal was digitally rectified, integrated for 0.5 ms ( $EMG_{ave}$ ), sampled at 200 Hz, and finally filtered (25-ms moving average window). This signal was denoted  $EMG_{ma}$ .

$$EMG_{ma}(t) = \frac{1}{5} \sum_{i=-2}^2 EMG_{ave}(t-i) \quad (11)$$

The  $EMG_{ma}$  signals were used as the input signals in (1), i.e.,  $EMG$ .

### 3.2 Experiment 2: movement generation

These measurements of arm positions and EMG signals were simultaneously continued during movements and maintenance of posture using the same method as in experiment 1. Again, the subject's wrist was secured by a cuff and supported horizontally. In Fig. 4, the target positions are indicated by the black diamonds.  $T_1$  to  $T_6$  are starting and ending positions, and  $P_1$  and  $P_2$  are

Table 1. Parameters of the human arm

	Link 1 (upper arm)	Link 2 (forearm)
$L_i$ [m]	0.256	0.315
$l_{gi}$ [m]	0.104	0.165
$M_i$ [kg]	1.02	1.16
$I_i$ [kg m <sup>2</sup> ]	0.0167	0.0474

via points (see Uno et al. 1989a). The subject was asked to produce five different unrestrained point-to-point movements between the five targets, i.e.,  $T_3 \rightarrow T_6$ ,  $T_2 \rightarrow T_6$ ,  $T_1 \rightarrow T_3$ ,  $T_4 \rightarrow T_1$ ,  $T_4 \rightarrow T_6$ ; movements were repeated in the opposite direction. Then the subject made via-point movements between two targets in the horizontal plane. Two cases,  $T_3 \rightarrow P_1 \rightarrow T_5$ ,  $T_3 \rightarrow P_2 \rightarrow T_5$ , were tested in both directions. The movement durations ranged from about 600 ms to about 800 ms. Each of the 14 movements consisted of 10 trials. During movement, joint angular velocity and acceleration were computed using numerical differentiation. The joint torques were calculated from the trajectories using the dynamics equations (10), because dynamical torques cannot be measured directly during movement.

### 3.2.1 The physical parameters of the subject arm

The physical parameters of the arm of a human subject were calculated from its 3D shape. First, the shape of the subject arm was scanned in 3D space by the Cyberware Laser Range Scanner. Then, assuming a uniform material with a specific gravity of 1.0, the mass, the center of mass, and the rotary inertia were calculated from the cubic volume. The density of water is a good approximation both for soft and hard tissues. Table 1 shows the estimated physical parameters of the subject arm for the (10).

### 3.3 Experiment 3: posture maintenance

In experiment 3, the subject produced co-contraction of muscles while maintaining the same posture without exertion of force at 23 points over the workspace indicated by the white squares. Thus, the net torques generated were 0. Three trials at each point lasted for 6 s and were of various co-contraction levels.

## 4 Simulation results

### 4.1 Joint torque estimation using an artificial neural network model

In order to train the network, the popular back-propagation algorithm (Rumelhart et al. 1986) in conjunction with the steepest ascent method was examined first. Because its rate of convergence is slow, we used the kick-out method (Ochiai and Usui 1994) in which learning rates are adjusted according to the rate of increase in the objective function during the last few steps.

#### 4.1.1 Estimation of the weights between the first and second layers (filter)

To specify the relationship between EMG signals and quasi-tension, joint torques under isometric conditions measured in experiment 1 were first estimated from surface EMG signals using a simple, nonmodular, four-layer neural network such as shown in Fig. 3. The network was trained with the odd-numbered trials from experiment 1, and the even-numbered trials were used for a cross-validation test. The training employed 10000 sample points from  $5.0 \text{ s} \times 10 \text{ trials} \times 200 \text{ Hz}$  sampling rate ( $10000 = 5 \times 10 \times 200$ ). The weights between the first layer and second layer after learning are shown in Fig. 6. The

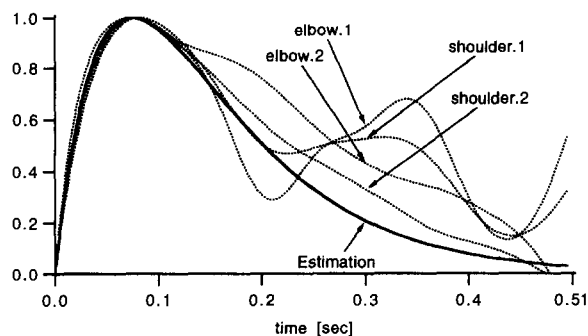


Fig. 6. Impulse response of the second-order temporal filter which determines the quasi-tension from EMG. The ordinate scale is arbitrary with the peak response of 1.0

dotted lines for shoulder.1 and elbow.1 indicate weights obtained from a previous study using the same subject (Koike et al. 1992). The dotted lines for shoulder.2 and elbow.2 indicate the weights obtained this time. The coefficients of (3) were estimated from shoulder.1 and elbow.1 using the least squares error method for 0.25 s. A comparable calculation for 0.5 s yielded weights which were less stable and variable for different joints. The solid line in Fig. 6 shows the resulting impulse response with  $a = 6.44$ ,  $b = 10.80$ , and  $c = 16.52$  in (3). Using these coefficients, the isometric torques were estimated accurately. Because the coefficient of determination (square of the correlation coefficient between actual torques and estimated torques) for the test data was 0.897 and, moreover, shoulder.2 and elbow.2 which were obtained from the present experiment fit the estimated impulse response well, we can conclude that the obtained filter was reliable. The coefficients  $a$ ,  $b$ , and  $c$  of the filter were fixed when the torques were estimated during movement in the next step.

Figure 7 shows EMG signals  $EMG_{ma}$  calculated from (11), and quasi-tension  $\hat{T}$  given by (1). We can see that the quasi-tension signal (smooth curve) lags about 100 ms behind the  $EMG_{ma}$  signals.

#### 4.1.2 Estimation of the weights between the second and fourth layer (nonlinear transformation)

Next, data from experiments 2 and 3 explained in Sects. 3.2 and 3.3 were used to finally determine the

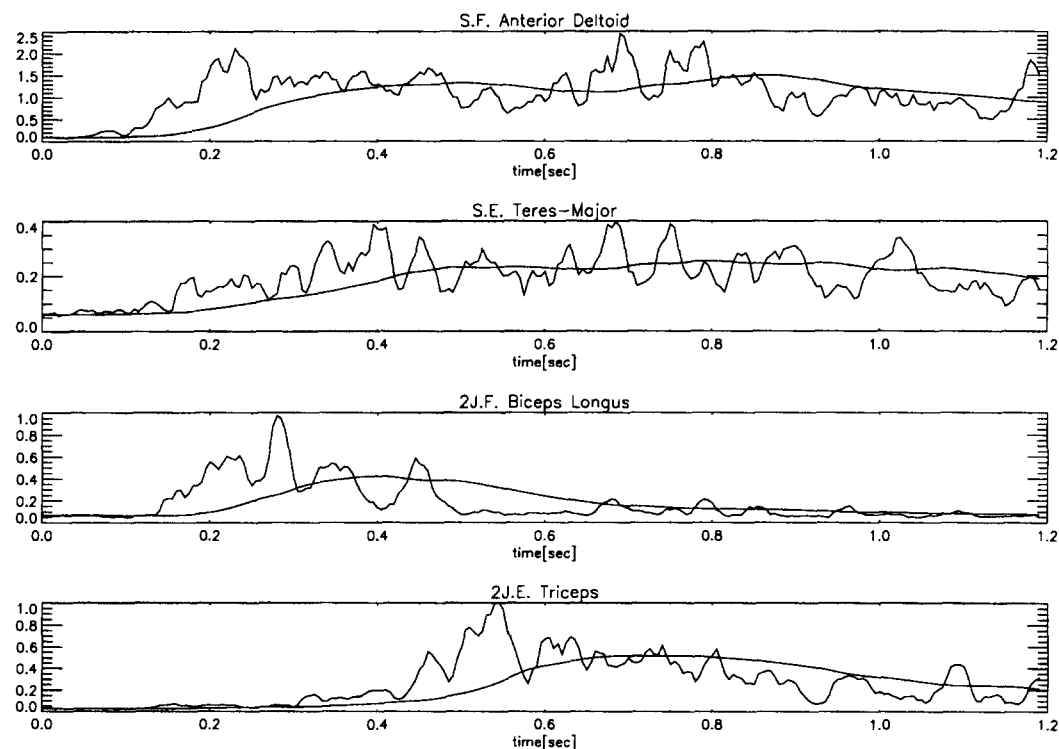


Fig. 7. Measured EMG signals and quasi-tension for the four muscles (DLC, TEM, BIL, TRL)

weights between the second and fourth layers. Thus, nonlinear properties of the musculoskeletal system were evaluated from the data of movements and posture maintenance without exerted forces. The network was trained with the odd-numbered trials from experiment 2, and the even-numbered trials were used for a cross-validation test. The training employed 35 000 sample points ( $2.5 \text{ s} \times 70 \text{ trials} \times 200 \text{ Hz}$  sampling rate).

The data from the first and third trials for posture control from experiment 3 were also used to train the network. In this case, the target dynamic torque is zero because no movement or exerted force was generated in experiment 3. The second trial was saved for a performance test. The training employed 50 600 sample points ( $5.5 \text{ s} \times 46 \text{ trials} \times 200 \text{ Hz}$  sampling rate). The test employed 25 300 sample points ( $5.5 \text{ s} \times 23 \text{ trials} \times 200 \text{ Hz}$  sampling rate). The learning was broken off before the error in the test data began to increase (cross validation method; Wada and Kawato 1992). This is the standard way of cross-validation to avoid 'over learning' in which synaptic weights are tuned too much to the training data, and generalization capability is lost. This was routinely used for all training sessions.

Before modular learning, the approximate torque estimation network and the gating network were trained using both movement and posture data. Expert network 1 was pretrained using the posture maintenance data from experiment 3. In contrast, expert network 2 was pretrained using the movement data from experiment 2. After prelearning, modular learning was done with the values of 0.05 for both  $\sigma_1$  and  $\sigma_2$  in (6) using both moving and stationary position data. The purpose of pretraining of the gating, expert, and approximate torque estimation networks is to lay 'seeds' in those network weights before the usual modular learning takes place. Good initial synaptic weights obtained by this pretraining greatly enhanced automatic division of two expert networks as well as dramatically reduced the overall learning time.

Figure 8 shows one example of the estimation result of the joint torques for the shoulder and elbow (upper traces) and the output of the gating network for test data

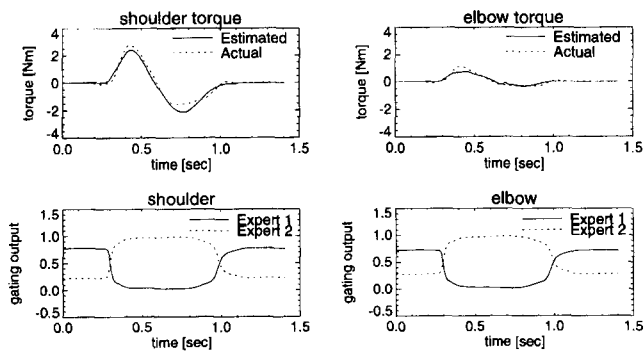


**Fig. 8.** Estimation results of joint torques for shoulder (left) and elbow (right). Dotted curves show the actual torque, and solid curves show the estimated torque in the upper row; solid curves show results for expert 1, and dotted curves show results for expert 2 in the lower row

(lower traces). Prediction was made at each time step from the position, velocity, and EMG data from the test set. As far as the torque is concerned, the dotted line is for the actual torque, and the solid line is for the network output. For the output of the gating network, the solid line corresponds to expert 1, and the dotted line corresponds to expert 2. Overall for test data from experiments 2 and 3, the determination coefficient of dynamic torque was 0.887. Thus, the dynamic torques were reliably predicted by our proposed network. Expert 1's output corresponds to 'posture', and expert 2's output corresponds to 'movement'. From the lower trace of Fig. 8, we can assert that the gating network switched the expert networks correctly for both the stopping and moving conditions.

#### 4.2 Trajectory formation

The trajectories were calculated from the initial position and velocity and the continuous EMG signals for point-to-point movements and via-point movements. This was done in the following recursive way.

- Step 1. At each time step, the dynamic torque was predicted by the neural network model from the position and velocity values at the current time step and the past 500 ms of EMG data. Then this predicted torque was used as the control input to the dynamics equations (10).
- Step 2. Numerical integration of (10) by Euler's method from the current values of the position, velocity, and torque provides the next step value of position and velocity.

These two steps were repeated until the end of the recording duration. Figure 9 shows one example of the simulation results of trajectory generation for  $T_3$  to  $T_6$ . In descending order, the joint angle, angular velocity, angular acceleration, torque, and output of the gating network are shown. The left column corresponds to the shoulder and the right one to the elbow. In the upper 4 rows, the solid curve is the network output, and the dotted curve is the experimental data. In the bottom row, the solid curve is the output for expert 1, and the dotted curve is the output for expert 2. Similar to the one-step prediction described before, the gating network switched the expert networks correctly for both the stopping and moving conditions. It should also be noted that at the start and end of a movement, the output of the gating network began to change in advance of the velocity change, allowing the expert network output to follow.

Figure 10 shows trajectories on the  $X$ - $Y$  plane. Overall, for test data shown in Fig. 10 from experiment 2, the coefficient of determination for position data predicted from initial conditions of position and velocity and EMG time course is 0.948. Therefore, even though there was a gradual accumulation of error because the angle and angular velocity at the next time step were recursively calculated by summing the predicted accelerations with the current angular velocity, the trajectories were reconstructed accurately. Some trajectories on the  $X$ - $Y$  plane

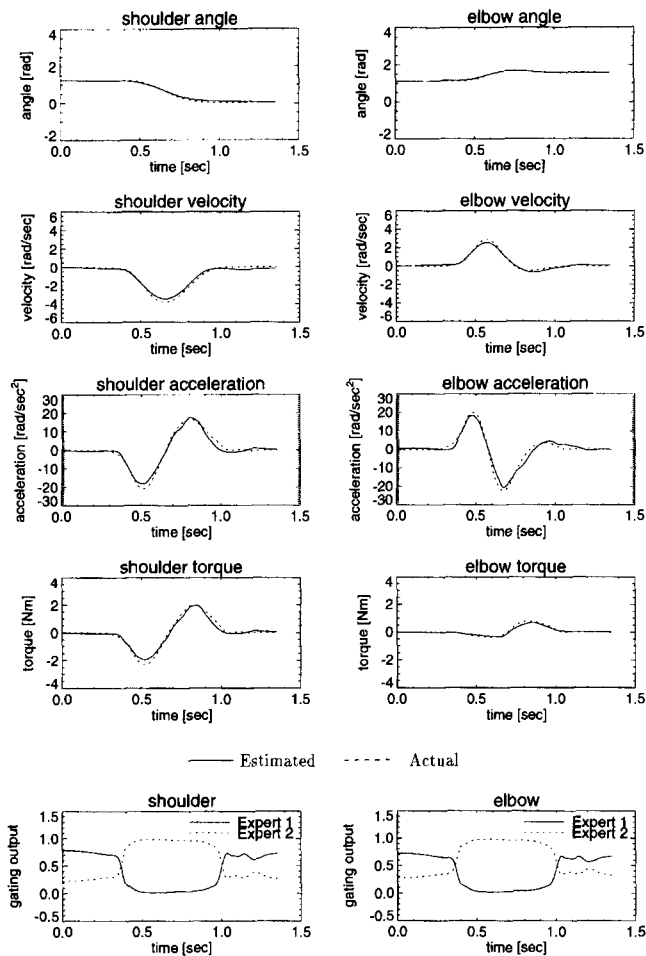


**Fig. 9.** Joint angle (*first row*), angular velocity (*second row*), angular acceleration (*third row*), and joint torque (*fourth row*) predicted during point-to-point movement. *Dotted curves* show actual values, and *solid curves* show estimated values in the *upper four rows*. The *bottom row* shows the outputs of the gating network. Here, *solid curves* show the output of the gating network for expert 1, and *dotted curves* show the output of the gating network for expert 2

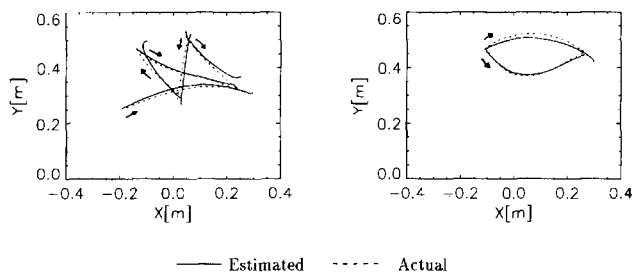


**Fig. 10.** Calculated trajectories on X-Y plane. *Dotted curves* show actual and *solid curves* estimated paths

were slightly different from the actual trajectories because of the error accumulation. There is, however, almost no significant error for the joint angle. This is the first demonstration that multijoint movements and posture maintenance can be fairly accurately predicted from

multiple surface EMG signals while allowing complicated via-point movements as well as co-contraction.

## 5 Discussion

Joint torques and then human arm movements have been estimated from surface EMG signals using a four-layer artificial neural network with a modular architecture. In the implementation, we took account of the following domain-specific knowledge: (1) the relationship between the EMG input signal and quasi-tension; (2) the dynamics of the arm; and (3) nonlinear muscle properties. To implement (1), a network was prepared to work as a temporal FIR filter between the first and second layer. For this filter, we found about a 100-ms lag between EMG signals and quasi-tension. Soechting and Roberts (1975) reported the natural frequency of the impulse response relating EMG to force of human muscle was 2.5 Hz. Moreover, Bawa and Stein (1976) reported that the natural frequency of the impulse response for the human soleus muscle was around 2 Hz. These natural frequencies correspond to about a 60- to 100-ms delay between EMG signals and muscle tension. Bennett (1993) also pointed out this low-pass property of muscles and reported delays of approximately 60–90 ms between surface EMG signals and human arm muscle tension. To implement (2), the physical parameters of the subject arm were calculated from the measured 3D shape of the arm, and the arm dynamics were described by lagrangian equations. Furthermore, some nonlinear properties of the musculoskeletal system were obtained by training the neural network; expert networks were trained separately from training data focusing on movement or posture control to efficiently implement (3). There are several reasons for using two expert networks. For example, from the physiological viewpoint, the use of muscles differs depending on whether the arm moves or not. When the arm is moving, the relationship between velocity and tension has to be considered. In the case of posture control, however, the velocity-tension relationship does not need to be considered. It is also widely known that the dynamic characteristics of spinal and supraspinal reflex loops differ widely between movement and posture maintenance. The approximate torque estimation network was added to calculate joint torques to provide the information useful for the gating network.

Until now, mainly qualitative descriptions have been made regarding the relationship between movements and EMG, such as recognizing registered movement patterns from surface EMG signals (Suzuki and Suematsu 1969; Mori et al. 1992). In this paper, however, trajectories were estimated quantitatively from surface EMG signals. The complexity of musculoskeletal systems makes it difficult to reconstruct movement trajectories accurately from EMG signals. We use point-to-point movements or via-point movements in the horizontal plane, which almost covered the workspace. Also, the link dynamics is not simple because of the presence of complex interaction forces among moving link segments.

The comparison of the estimated and measured trajectories is a severe test of the goodness-of-fit of the model because it is essential to estimate the shoulder and elbow joint torques not only qualitatively but also quantitatively to reconstruct trajectories accurately. We have also confirmed that each joint torque was accurately reconstructed by comparing the estimated torque waveforms and data torques as shown in Fig. 8. Moreover, the model was examined by using the test data which were not employed for training: this is further confirmation of the generalization capability of the model.

The constructed forward dynamics model can serve as a fundamental tool for the computational study of multijoint arm movements. Other than this scientific use, several engineering applications might also be possible. For example, by using the network, EMG signals could be used as human interface inputs to control a 'virtual arm' in a virtual reality environment. A further possibility is for the motor command produced by a minimum-muscle-tension-change model (Uno et al. 1989b) based on the neural network forward dynamics model to be applied to a paralyzed limb.

Regarding computational studies of motor control based on the acquired forward dynamics model, our future work includes (1) calculating of virtual trajectories to critically examine the virtual trajectory hypothesis (see Koike and Kawato 1993 for preliminary results), (2) learning the inverse dynamics model, and (3) examining a minimum-motor-command-change model (Kawato 1992).

*Acknowledgements.* We thank Dr. F. Kishino and N. Wada of ATR Communication Systems Research Laboratories for their help in measuring the 3D shape of the human arm. We are grateful to D.J. Ostry, F.E. Pollick, E.V. Bateson and K.G. Munhall for their editing of the first draft of this paper. The work was partly supported by Human Frontier Science Program grants to M.K.

## References

- Akazawa K, Takizawa H, Hayashi Y, Fujii K (1988) Development of control system and myoelectric signal processor for bio-mimetic prosthetic hand. *Biomechanism* 9:43-53
- Basmajian JV, De Luca CJ (1985) *Muscles alive*. Williams & Wilkins, Baltimore
- Bawa P, Stein R (1976) Frequency response of human soleus muscle. *J Neurophysiol* 39:788-793
- Bennett D (1993) Electromyographic responses to constant position errors imposed during voluntary elbow joint movement in human. *Exp Brain Res* 95:499-508
- Brown S, Cooke J (1990) Movement related phasic muscle activation. I. Changes with temporal profile of movement. *J Neurophysiol* 63:455-464
- Clancy EA, Hogan N (1991) Estimation of joint torque from the surface EMG. Annual International Conference of the IEEE Engineering in Medicine and Biology Society 13:0877-0878
- Dornay M, Uno Y, Kawato M, Suzuki R (1992) Simulation of optimal movements using the minimum-muscle tension-change model. In: Moody JM, Hanson SJ, Lippmann RP (eds) *Advances in neural information processing systems 4*. Morgan Kaufmann, San Mateo, pp 627-634
- Gottlieb GL, Corcos DM, Agarwal GC (1989) Organizing principles for single-joint movements. I. A speed-insensitive strategy. *J Neurophysiol* 62:342-357
- Jacobs R, Jordan M (1991) A competitive modular connectionist architecture. In: Moody JM, Hanson SJ, Lippmann RP (eds), *Advances in neural information processing systems 3*. Morgan Kaufmann, San Mateo, pp 767-773
- Karst G M, Hasan Z (1991) Timing and magnitude of electromyographic activity for two-joint arm movements in different directions. *J Neurophysiol* 66:1594-1604
- Katayama M, Kawato M (1993) Virtual trajectory and stiffness ellipse during multijoint arm movement predicted by neural inverse models. *Biol Cybern* 69:353-362
- Kawato M (1992) Optimization and learning in neural networks for formation and control of coordinated movement. In: Meyer D, Kornblum S (eds), *Attention and performance, XIV*. MIT Press, Cambridge, Mass.
- Koike Y, Kawato M (1993) Virtual trajectories predicted from surface EMG signals. *Soc Neurosci Abstr* 19:543
- Koike Y, Kawato M (1994a) Estimation of arm posture in 3D-space from surface EMG signals using a neural network model. *IEICE Trans Fundamentals D-II(4)*:368-375
- Koike Y, Kawato M (1994b) Trajectory formation from surface EMG signals using a neural network model. *IEICE Trans (D-II)* J77(1):193-203 (in Japanese)
- Koike Y, Honda K, Hirayama M, Gomi H, Bateson E-V, Kawato M (1992) Dynamical model of arm using physiological data. *Tech Rep IEICE NC91-146*, pp107-114 (in Japanese)
- Koike Y, Honda K, Hirayama M, Gomi H, Bateson E-V, Kawato M (1993), Estimation of isometric torques from surface electromyography using a neural network model. *IEICE Trans (D-II)* (6):1270-1279 (in Japanese)
- Mannard A, Stein R (1973) Determination of the frequency response of isometric soleus muscle in the cat using random nerve stimulation. *J Physiol* 229:275-296
- Mori D, Tsuji T, Ito K (1992) Motion discrimination method from EMG signals using statistically structured neural networks. *Tech Rep IEICE NC91-143*, pp 83-90 (in Japanese)
- Nowlan S, Hinton G (1991) Evaluation of adaptive mixtures of competing experts. In: Moody JM, Hanson SJ, Lippmann RP (eds), *Advances in neural information processing systems 3*. Morgan Kaufmann, San Mateo, pp 774-780
- Ochiai K, Usui S (1994) Kick-out learning algorithm to reduce the oscillation of weights. *Neural Networks* 7:797-807
- Rack P, Westbury D (1969) The effects of length and stimulus rate on tension in the isometric cat soleus muscle. *J Physiol* 217:419-444
- Rumelhart D, Hinton G, Williams R (1986) Learning representations by backpropagating errors. *Nature* 323:533-536
- Soechting J, Roberts W (1975) Transfer characteristics between EMG activity and muscle tension under isometric conditions in man. *J Physiol* 70:779-793
- Suzuki R, Suematsu T (1969) Pattern recognition of multi-channel myoelectric signals by learning method. *Jpn J Med Electron Biol Eng* 7:47-48 (in Japanese)
- Uno Y, Kawato M, Suzuki R (1989a) Formation and control of optimal trajectory in human multijoint arm movement: minimum torque-change model. *Biol Cybern* 61:89-101
- Uno Y, Suzuki R, Kawato M (1989b) Minimum-muscle-tension-change model which reproduces human arm movement. *Proceedings of the 4th Symposium on Biological and Physiological Engineering*, pp 299-302 (in Japanese)
- Wada Y, Kawato M (1992) A new information criterion combined with cross-validation method to estimate generalization capability. *Syst Comput Jpn* 23:92-104
- Winters JM (1990) Hill-based muscle models: a systems engineering perspective. In: Winters JM, Woo SL-Y (eds), *Multiple muscle systems*. Springer Berlin Heidelberg New York, pp 69-93
- Wood J, Meek S, Jacobsen S (1989) Quantitation of human shoulder anatomy for prosthetic arm control. II. Anatomy matrices. *J Biomech* 22:309-325.